Tornadogenesis in High-end Tornadic Supercells (Part 3)
Moore, Oklahoma EF5 on May 20, 2013
A Case Representative of Tornadogenesis

Chris Broyles[1], Corey Potvin[2], Greg Dial[1], James Murnan[2], Steven Shores[4], Andrew Lyons[1], Matthew Elliott[1], Ashton Robinson Cook[3]

[1] NOAA/NWS/NCEP/Storm Prediction Center, Norman, Oklahoma
[2] NOAA/National Severe Storms Laboratory, Norman, Oklahoma
[3] Weather Prediction Center, [4] University of Oklahoma Student

Abstract

A database of 208 supercells that produced tornadoes rated EF3 to EF5, was created at the Storm Prediction Center for examining and better understanding tornadogenesis. Using WSR-88D high-resolution radar, 113 data characteristics were gathered for each supercell related to tornadogenesis. After enough storms were analyzed, a conceptual model of tornadogenesis began to emerge from these radar observations. The average times of key events, leading up to the tornado and during its development, were calculated. From there, an animation was created showing those key events. Over time, the animation was adapted to the processes that were observed on radar for the Moore EF5 supercell on May 20, 2013.

As data was being gathered for the 208 supercells, an algorithm was developed to assess how close each storm was to the database average concerning tornadogenesis. 14 categories were chosen for the calculation that would rank each storm. Those 14 categories were associated with the rear flank downdraft surge, inflow channel, descending reflectivity core, cell mergers and inflow connection. Using the ranking method, the Moore, Oklahoma EF5 supercell on May 20, 2013, was closest to the 208 case average. Based on that result, the Moore, Oklahoma EF5 tornadic supercell is a representative storm for better understanding tornadogenesis in storms that produce tornadoes in the EF3 to EF5 range. This paper covers the processes that were discovered during the radar analysis for the Moore EF5 supercell. These processes are discussed in great detail using drawings from the animation. This paper uses the hand-drawn animation with radar inserts to show the complete life cycle of the Moore, Oklahoma EF5 tornado on May 20, 2013.

1. INTRODUCTION

The topic of tornadogenesis has been intensely studied for decades, and much progress has been made. Over the years, case studies and field observations have identified many of the features associated with tornadogenesis in supercells. Some of those features include the rear flank downdraft (RFD), forward flank downdraft (FFD), hook echo, RFD surge, descending reflectivity core (DRC), inflow channel and cell mergers.

Around and before the turn of the century, concerning research on this topic, some of the more prominent publications include Lemon and Doswell 1979, Klemp and Rotunno 1983, Markowski 2002, Rasmussen et al. 2006, Davies-Jones 2006, Wurman et al. 2007 and Finley et al. 2010. In recent years, some important publications on this topic include Lee et al. 2012, Kosiba et al. 2013, Atkins et al. 2014, Burgess et al. 2014, Ortega et al. 2014, Kurdzo et al. 2015, Dixon et al. 2018, Orf et al. 2018 and Satrio 2019. Our goal for this study is to build upon the research that has already been done, and to learn more how the various supercell features contribute to the formation of high-end tornadoes, in frequency, timing and causation.

2. METHODOLOGY

To study tornadogenesis, a large database was created consisting of 208 supercells that produced EF3 to EF5 tornadoes. An archive of high-resolution radar at the Storm Prediction Center was used to analyze each storm. Key events in tornadogenesis were examined including the RFD surge, RFD occlusion, descending reflectivity core, cell merger, inflow channel and inflow connection. After analysis was done for the first 26 storms in the database, the examination of radar was halted due to the pandemic. At that time, averages had already been computed for the key events related to tornadogenesis for those 26 tornadic supercells. At the beginning of October 2020, the lead author decided to start a side project, drawing a series of images that mirror tornadogenesis according to the averages obtained for the key events. The lead author worked for 12 hours per day for the first three months (October to December), drawing a highly detailed animation of tornadogenesis.

By the end of this time period, the initial version of the animation was complete for a hypothetical supercell. The animation consisted of a supercell, RFD surge, RFD occlusion, inflow channel and tornado. The tornado life cycle was shown with air motions drawn in around the tornado, to give the viewer an understanding of how and why tornado intensity fluctuated. The animation ended after the tornado diminished.

After this initial animation, a search was made for a storm to which the animation could be adapted. The storm had to be close to the average, so that the animation could be easily adapted. After examining the Moore, Oklahoma EF5 tornadic supercell on May 20, 2013, it turned out to be a very good match. The animation was then adapted specifically to the Moore EF5 supercell. Although the processes were similar, the adaptation was still an incredibly complex endeavor.

From January to May of 2021, work slowed to about 4 hours per day. During June 2021, the first animated version of the Moore EF5 supercell was complete. In the fall of 2021, work restarted to show the development of the cumulonimbus associated with the Moore EF5 supercell. Work continued through the summer of 2022 until the animation was finished in October 2022 after 25 months of work. The hand-drawn animation took an estimated 2,800 hours to complete. Together, the radar analysis for the 208 tornadic supercell database and the animation of the Moore, Oklahoma EF5 tornadic supercell, took a total of approximately 4,300 hours.

Due to the pandemic, only 26 storms had been analyzed as of the summer of 2021. During the fall of 2021, the analysis of the 208 tornadic supercells was restarted. During the winter of 2021-2022, work accelerated. After 60 storms were analyzed, an algorithm was designed to determine how close any one supercell in the database was to the database average. Fourteen categories were chosen for the algorithm, including RFD surge type, RFD surge start time, RFD surge end time, RFD surge duration, RFD surge speed, RFD surge direction, descending reflectivity core characteristic, cell merger one start time, cell merger two start time, cell merger three start time, inflow connection time, inflow channel start time, inflow channel end time and inflow channel duration.

To determine how close a storm was to the average, first the database average for each individual category was copied into a spreadsheet. The times for each category for each storm were subtracted from the database average, to obtain an absolute value for how close that storm was to the 208 case average. Then, the storms were sorted and ranked for each category. After all computations were done, the ranks for all 14 categories were added together for each storm. Finally, the total for each storm was sorted and ranked, from the lowest score (closest to the average) to the highest score (furthest from the average). The first ranking after 60 storms, had the Moore EF5 supercell on top as the closest storm to the tornadogenesis average. By the time all 208 storms were analyzed in the spring of 2022, the Moore EF5 supercell maintained its number one ranking.

Figure 1 shows the rankings for all 208 storms, with the closest storm to the average at the left and the furthest storm from the average at the right. At the left, 12 of the top 25 (48%) high-end supercells produced violent tornadoes (EF4 to EF5), while at the right, only three of the bottom 25 (12%) did so. And 41.4% of the top 70 supercells produced violent tornadoes, while 20% of the bottom 70 supercells did so. Based on this dataset, if a high-end supercell is close to the tornadogenesis average, then a violent tornado is considerably more likely than if a supercell is far away from the tornadogenesis average. Basically, the more organized a tornadic supercell becomes, the more likely a violent tornado can be produced.

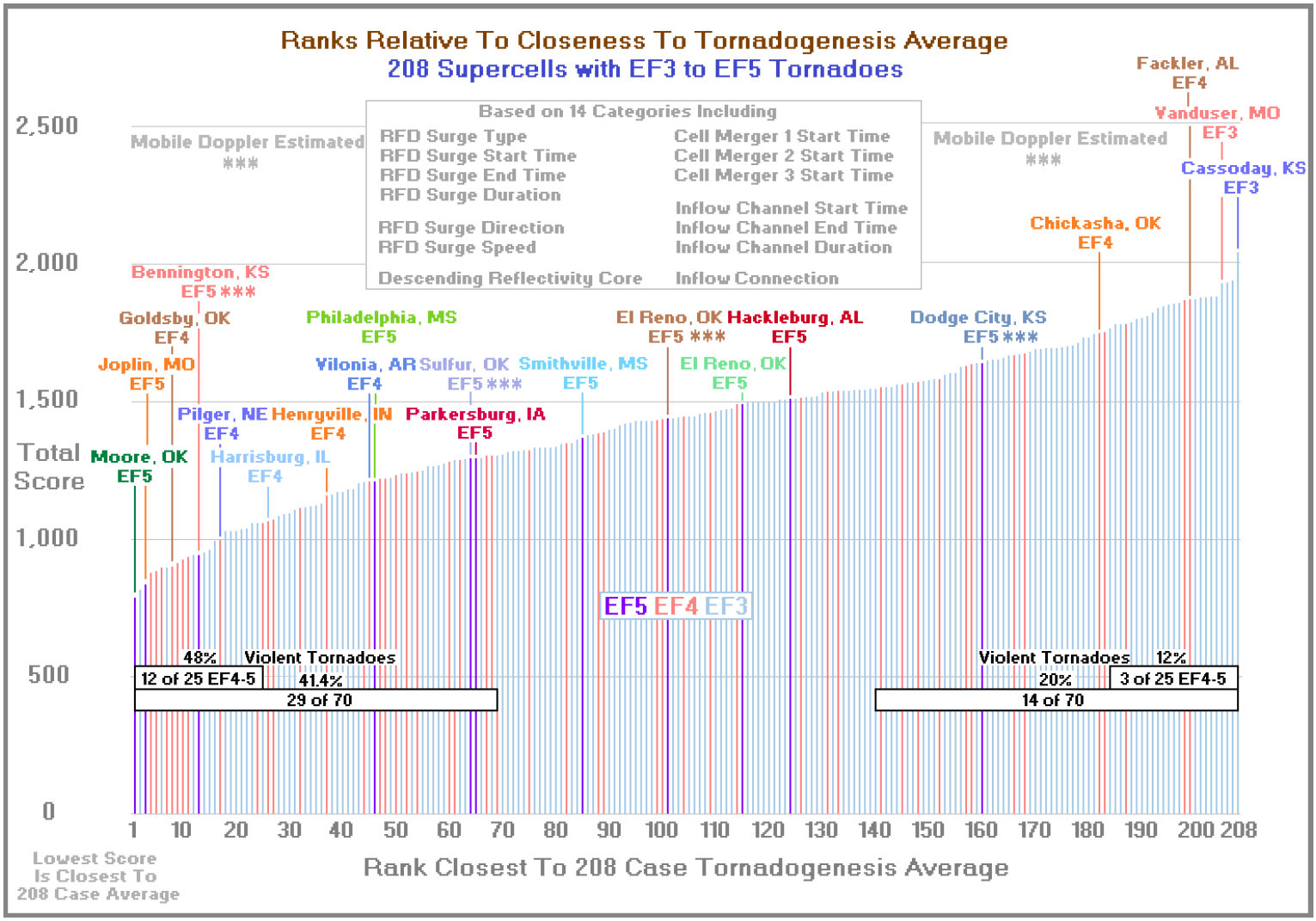

Figure 1. Ranks for how close each supercell was to the 208 case average for 14 categories associated with tornadogenesis. Those 14 categories are listed at the top of the graphic. The EF scale for each tornado is colored purple for EF5, pink for EF4 and light blue for EF3. Tornadoes that achieved an unofficial EF5 rating based on mobile Doppler radar have asterisks. The Moore, Oklahoma EF5 tornadic supercell was the number one storm closest to the 208 case average. Twelve of the top 25 (48%) supercells had violent tornadoes (EF4-EF5), while three of the bottom 25 (12%) had violent tornadoes. This shows predictability. If a high-end supercell is close to the tornadogenesis average, then a violent tornado is considerably more likely than if it is far from the tornadogenesis average.

TOP 20 CLOSEST STORMS TO 208 STORM TORNADOGENESIS AVERAGE

Rank	Rating	Day	Town	State
1	EF5	May 20, 2013	Moore,	OK
2	EF3	Apr 27, 2011	Bellafontaine,	MS
3	EF5	May 22, 2011	Joplin,	MO
4	EF4	June 11, 2008	Manhattan,	KS
5	EF4	May 9, 2016	Katie,	OK
6	EF3	May 10, 2010	Pink,	OK
7	EF4	Apr 28, 2014	Louisville,	MS
8	EF4	May 24, 2011	Goldsby,	OK
9	EF4	June 25, 2010	Sibley,	IA
10	EF4	May 10, 2010	Moore,	OK
11	EF4	Apr 27, 2011	Wetumpka,	AL
12	EF3	May 23, 2008	Clark State Lake,	KS
13	EF5	May 28, 2013	Bennington,	KS ***
14	EF3	Apr 19, 2011	Girard,	IL
15	EF3	May 28, 2013	Corning,	KS
16	EF3	Apr 24, 2010	Mentone,	AL
17	EF4	June 16, 2014	Pilger,	NE
18	EF3	May 9, 2016	Connerville,	OK
19	EF3	Apr 28, 2014	Crawford,	AL
20	EF3	Apr 28, 2014	Tupelo,	MS

*** EF5 Mobile Doppler Estimated

The top 20 storms closest to the 208 case tornadogenesis average are listed above. Of the top 20, there are three EF5s on the list including the Moore, Oklahoma EF5 #1, the Joplin, Missouri EF5 #3 and the Bennington, Kansas EF5 #13. The Bennington, Kansas tornado was officially rated EF3 on the damage survey but achieved an unofficial EF5 rating using mobile Doppler radar. These three storms are excellent case studies in order to better understand tornadogenesis. The Moore, Oklahoma EF5 supercell was selected for a comprehensive examination using all data possible, with high-resolution radar being used as the primary source of data. According to this study's ranking method, the Moore EF5 supercell is representative of the processes observed in tornadogenesis for this dataset. In addition to this study, a detailed analysis of the Moore EF5 supercell is presented in Atkins et al. 2014, Kurdzo et al. 2015 and Satrio 2019.

3. MOORE EF5 ANIMATION

The Moore, Oklahoma EF5 supercell animation includes the development of the supercell and the entire lifecycle of the tornado. It can take between two and four minutes to view, depending upon how fast the user wants to view the frames. In addition to the illustrations, there are radar images inset at the top right that show the events taking place.

There is also a table at the top right that shows various pieces of data that were measured by radar, including rotational velocity (VROT), meso diameter in nautical miles, descending reflectivity core wind speed in knots, RFD surge speed in knots, inflow channel maximum wind speed in knots, inflow sector wind speed in knots, surface pressure, surface wind speed in miles per hour and 700 mb wind speed in knots.

All the values were estimated using measurements by radar except for CAPE, which was a manually calibrated estimate. The CAPE values are consistent with the May 20, 2013 18Z sounding from Norman, Oklahoma. Archived mesoscale analysis from the Storm Prediction Center was used to calibrate the CAPE values. CAPE was also calibrated by the RFD study on the Bowdle, South Dakota EF4 tornado that occurred on May 22, 2010 (Finley et al. 2010).

The other wind speed estimates were made using a technique in which supercell streamline analysis was done to estimate the wind direction. An adjustment was made to the wind speed based on the determined angle of the wind to the radar beam. The wind speed for descending reflectivity core, inflow channel, inflow sector, 700 mb jet and occlusion downdraft were all determined using this method. The wind speed for the descending reflectivity core (DRC) is an estimate of the highest wind within the DRC as it descends to the surface.

The wind speed estimate for inflow channel is the maximum wind speed found in the inflow channel, averaging 888 feet above ground level. The wind speed estimate for the supercell's inflow sector is the average wind speed away from the inflow channel, averaging 732 feet above ground level. A sample of bins across the supercell's inflow sector was selected that appeared close to the average. Then, those bins were used to obtain the measurement.

The 700 mb wind speed was measured at a location 2.0 nautical miles and 140 degrees from the low-level mesocyclone, averaging 7,335 feet above ground level. While slightly below 700 mb, this height was considered sufficient to estimate the speed of the 700 mb jet. The scan elevation of the base velocity image for the 700 mb jet was 4.0 degrees.

The occlusion downdraft wind speed was estimated by finding the bin with the highest velocity just outside of the southern to eastern side of the tornado. The average height of the occlusion downdraft wind speed was 927 feet above ground level.

The surface wind is an estimate of the wind speed at ground level within the center of the low-level meso. It was determined by using 90 percent of the estimated inflow wind speed when there was no tornado. When the tornado was ongoing, the reported EF Scale and occlusion downdraft wind speed were used in an equation to estimate the surface wind speed. The occlusion downdraft wind speed was reliable because there were no data dropouts. VROT was not used to estimate surface wind speed because there were major data dropouts at key times in the life cycle of the tornado, suggesting that wind speeds at those times would be substantially underestimated.

The surface pressure was determined by the estimated ground level wind speed at the center of rotation. The resulting surface pressure graph is consistent with tornado pressure observations. The storm's speed of movement was determined for every 0.5 degree reflectivity image by measuring the distance traveled, using the nearest scan, 15 minutes before the image time to 15 minutes after. The times of all supporting data including radar images, mesocyclone measurements, wind measurements and photos are matched to the time of the nearest animation frame.

On the animation, the two radar images at the top right are reflectivity and storm relative velocity at the lowest elevation scan near or at 0.5 degrees. The radar images below the data table that show the individual processes are reflectivity and base velocity at the lowest elevation scan near or at 0.5 degrees, unless otherwise noted. When the animation was adapted to the May 20, 2013 case, the details of the animation were drawn to represent the Moore tornado as closely as possible. The width of the tornado was drawn to scale and all directional changes in the path were represented. Cloud cover across the Moore supercell's inflow sector was removed to enable viewing from above.

The animation of the Moore, Oklahoma EF5 tornadic supercell is 227 frames long. The animation begins at 18:26:00 Z on May 20, 2013 and ends at 20:47:15 Z, spanning 2 hours 21 minutes 15 seconds. Frames are 37.5 seconds apart. The animation begins looking north-northwest at 18:26 Z, from approximately 15,000 feet. During the next hour, a gradual transition is made from viewing north-northwest (335 degrees) to viewing west (265 degrees), as if looking from a helicopter that is repositioning.

The animation begins 20 minutes before the first cumulus develops for the Moore EF5 supercell. Convective initiation begins at 18:46:00 Z. Over the next 20 minutes, the cloud steadily grows. An anvil forms and spreads to the east-northeast as the updraft organizes. The Moore EF5 storm reaches supercell status at 19:06:00 Z, 20 minutes after convective initiation. The supercell continues to strengthen until a well-developed strong low-level mesocyclone is present 20 minutes later, at 19:26:00 Z. Over 12 minutes later at 19:38:30Z, and over 52 minutes after cell initiation, the process of tornadogenesis begins as two cells merge behind the Moore E5 supercell's flanking line. Two papers on tornadogenesis include Klemp and Rotunno 1983 and Davies-Jones 2006.

In the following pages, each stage of tornadogenesis will be covered for the Moore EF5 supercell. A discussion for each specific event associated with tornadogenesis will be made.

The corresponding frame with the actual event, will be shown from the animation. A comparison for each event will be made to the 208 case database. In each figure, the drawing seeks to accurately represent what the radar showed at that time. Tornadogenesis is complex and each stage will be presented in great detail. All event times are estimates based on radar. EF-scale data is based on Burgess et al. 2014 and Ortega et al. 2014.

INSTIGATION OF RFD SURGE BY A CELL MERGER

At 19:26:00 Z, convective initiation takes place behind the Moore EF5 supercell's flanking line. Over the next 12 minutes, two cumulus towers develop and move toward the back edge of the flanking line. Figure 2 shows the Moore EF5 supercell at 19:37:53 Z, with the two cells about to merge. The two cells merge 37 seconds later at 19:38:30 Z, constituting cell merger 1. Over the next 3 minutes 45 seconds, the enhanced outflow associated with cell merger 1, becomes absorbed into the flanking line. The outflow spreads east-northeastward, instigating the RFD surge at 19:42:15 Z (Figure 3).

For the Moore EF5 supercell, a cell merger likely instigated the RFD surge 13 minutes 45 seconds prior to the tornado start time. For the 208 case average, a cell merger instigated the RFD surge 13 minutes 31 seconds prior to the tornado start time. For the Moore EF5 supercell, the start of the RFD surge was remarkably close to the average. Another study looking at cell mergers and tornadogenesis is Wurman et al. 2007.

Moore, Oklahoma EF5 Supercell at 19:37:53 Z - 18 Minutes 7 Seconds Before Tornado

Impeding Cell Merger Behind Flanking Line Will Instigate RFD Surge

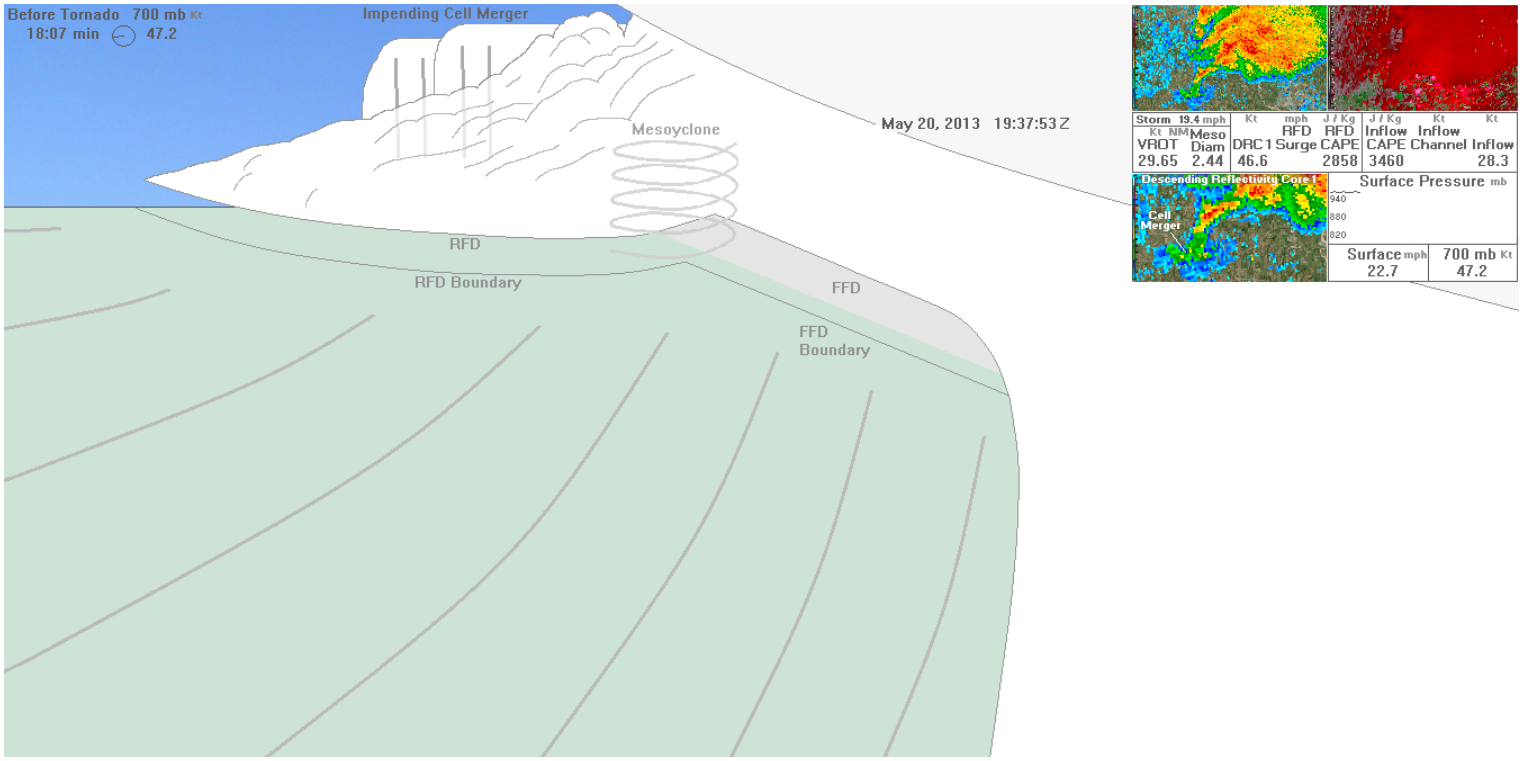

Figure 2. The Moore EF5 supercell at 19:37:53 Z. In 37 seconds, at 19:38:30 Z, a cell merger will happen behind the flanking line. The cell merger and the resultant outflow, will instigate the RFD surge after 3 minutes 45 seconds, at 19:42:15 Z.

MESO-BETA SCALE 700 MB JET

Another event happened that contributed to the RFD surge for the Moore EF5 supercell. This involved the 700 mb jet, which was analyzed specifically for this case. The 700 mb jet was not examined for the other 207 cases. For the Moore EF5 supercell, a meso-beta scale 700 mb jet was identified using high-resolution radar. Figure 3 shows the 700 mb jet hitting the flanking line from the south-southwest at 19:42:15 Z. The 700 mb jet shows up on the base velocity image (right middle) entitled "High 700 mb Speeds Approaching". Using high-resolution radar, wind speeds within the jet were estimated in the 60 to 80 knot range, while the environmental flow around the jet was approximately 50 knots. Radar estimates suggest the 700 mb jet was about 30 nautical miles long and about 8 nautical miles wide. The 700 mb flow was from 225 degrees (due southwest), while the 700 mb jet approached

the mesocyclone from 210 degrees, suggesting that the jet could have been associated with a wave in the low to mid-levels. The 700 mb jet was also likely being enhanced by relatively low-topped thunderstorms located upstream from the Moore EF5 supercell. Those storms were likely mixing higher wind speeds from above down to near 700 mb.

The dryline, cold front and triple point were all west of the Moore EF5 supercell. Several supercells were ongoing south-southwestward and north-northeastward of the Moore EF5 supercell. Yet none of the storms produced EF2+ tornadoes, except for the Moore supercell. This study hypothesizes that the 700 mb jet was the key ingredient, enabling the Moore supercell to produce the EF5 tornado.

While this type of meso-beta scale 700 mb jet is hard to observe, it is thought to occasionally occur for high-end tornadic supercells, mainly in environments when an extra boost in deep-layer shear is needed for high-end tornadogenesis. A similar feature may have been observed visually just prior to the EF4 tornado on May 28, 1996 in Bullitt County, Kentucky near Louisville.

The 700 mb jet for the Moore EF5 supercell not only rapidly strengthened the mesocyclone, it reinforced the RFD surge as well. The enhanced mid-level flow and cell merger caused the RFD surge to push out far into the inflow sector of the supercell, making conditions favorable for high-end tornadogenesis. This idea, that enhanced mid-level flow can strengthen the rear flank downdraft, is presented in Browning and Ludlam 1962, Browning and Donaldson 1963, Browning 1964, and Lemon and Doswell 1979.

Moore, Oklahoma EF5 Supercell at 19:42:15 Z - 13 Minutes 45 Seconds Before Tornado

Meso-beta Scale 700 mb Jet Hits Flanking Line - Reinforces RFD Surge - Rapidly Strengthens Mesocyclone

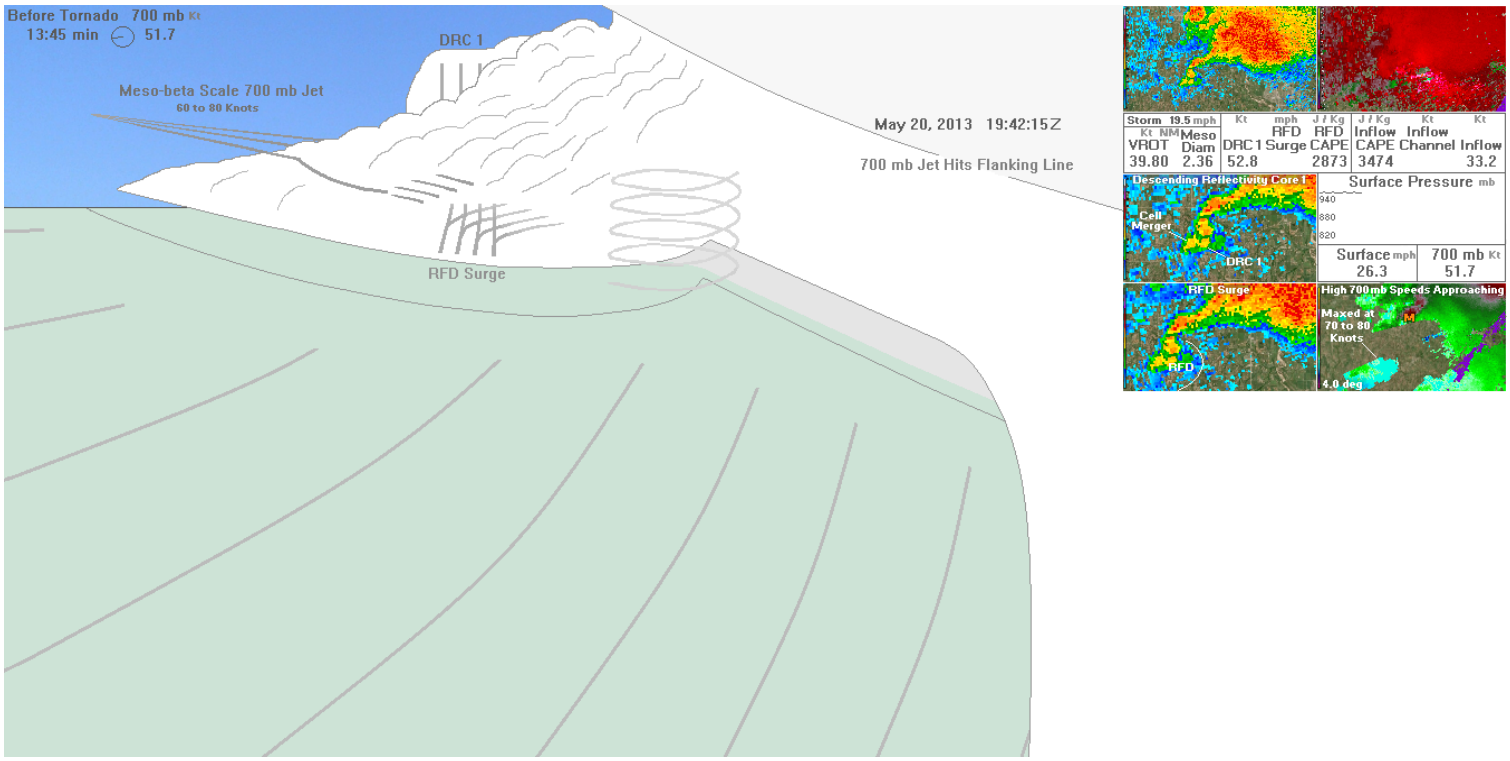

Figure 3. The Moore EF5 supercell at 19:42:15 Z. The RFD is surging beneath the flanking line due to cell merger 1. The RFD surge will push eastward and northward toward the supercell's forward flank. At this time, a meso-beta scale 700 mb jet has hit the flanking line and vertical shear is rapidly becoming favorable for a very strong mesocyclone. The 700 mb jet will cause storm rotation to rapidly increase over the next 10 minutes. The RFD surge is strengthened substantially.

RFD SURGE

The RFD surge began at 19:42:15 Z and ended at 19:59:45 Z. The duration was 17 minutes and 30 seconds. The 208 case average RFD surge duration was 17 minutes 53 seconds. The Moore EF5 supercell RFD surge duration was again close to the average. The RFD surge on the Moore EF5 supercell moved 6.6 knots faster than the parent supercell. This was close to the 208 case average of 6.9 knots.

In Figure 4, the RFD surge is still accelerating at 19:46:00 Z and is beginning to undercut the low-level mesocyclone. This will soon enable the RFD occlusion to form in the northeast quadrant of the RFD. The somewhat weaker low-level shear in the RFD will allow a column of vertical vorticity to organize without being torn apart.

Instability is now increasing within the RFD, as the RFD's leading edge moves out from beneath the flanking line. Sunshine is a bit more prevalent further ahead of the flanking line, allowing the RFD to destabilize more. At this time, DRC 1 is strengthening in the flanking line, just after the cell merger. DRC 1 is rapidly approaching the low-level mesocyclone from the west-southwest and will accelerate its descent to the surface in about 3 minutes. The 700 mb wind speed is now 67.4 knots.

Inflow channel development is imminent due to the RFD surge. The RFD surge and 60 to 80 knot 700 mb jet is setting the stage for rapid tornadogenesis. Other studies documenting multiple RFD surges and tornadogenesis in the Bowdle, South Dakota supercell are Finley et al. 2010 and Lee et al. 2012. Kosiba et al. 2013 documents the RFD within the Goshen, Wyoming supercell. And Markowski 2002 covers RFD observations relative to tornadogenesis.

Moore, Oklahoma EF5 Supercell at 19:46:00 Z - 10 Minutes Before Tornado

RFD Surge Continues To Accelerate - DRC 1 Strengthens Within Flanking Line Just After Cell Merger

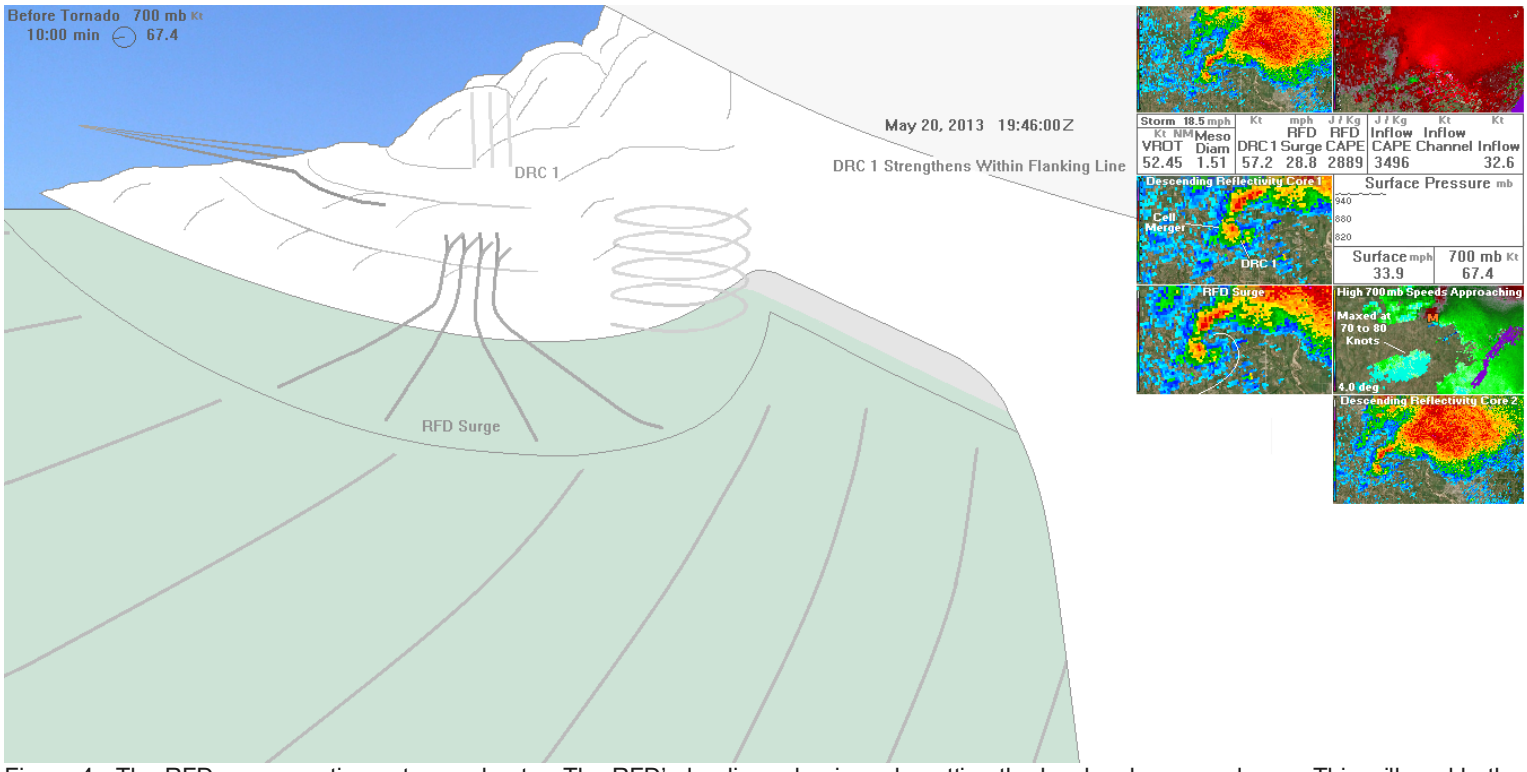

Figure 4. The RFD surge continues to accelerate. The RFD's leading edge is undercutting the low-level mesocyclone. This will enable the RFD occlusion to soon develop. Over the next few minutes, a column of vertical vorticity will begin to organize beneath the low-level mesocyclone. At this time, DRC 1 is rapidly approaching the low-level mesocyclone from the west-southwest. Instability within the RFD is beginning to rapidly increase as the RFD's leading edge pushes out from underneath the flanking line. Inflow channel development is imminent.

RFD OCCLUSION DEVELOPMENT AND MATURATION

In Figure 6 at 19:52:53 Z, the RFD occlusion is now fully matured. The RFD surge has reached its peak speed of movement at 24.4 knots (28.1 mph). The RFD occlusion began to develop 9 minutes 5 seconds before the tornado start time and reached a fully-developed state 4 minutes 49 seconds before the tornado start time. These times were fifth closest to the 208 case average. For the 208 cases, the RFD occlusion matured 4 minutes 37 seconds prior to the tornado start time. This is within 12 seconds of the Moore EF5 supercell's RFD occlusion maturation time.

At this time, DRC 1 and the occlusion downdraft rapidly descend toward the surface. The tornado will begin in 3 minutes 7 seconds as DRC 1 wraps into the RFD occlusion. Cells that will eventually produce DRC 2, and the associated outflow approach the Moore EF5 supercell from the southwest.

The inflow channel and streamwise vorticity current (SVC) are now developing. The SVC can be seen next to the inflow channel in the insert at the lower right. The peak wind speed within the inflow channel has increased to 62.9 knots due to the Bernoulli Effect.

The dramatic increase in inflow channel wind speeds will strengthen the low-level mesocyclone. As a result, upward vertical motion will increase, constituting the southern edge of the SVC. Air will flow over the top of the inflow channel. The pressure drop within the inflow channel will draw the forward flank downdraft into the inflow channel's center. This completes the SVC's horizontal rotational component.

The inflow channel and SVC are covered in detail in Part 2 of this study. A simulated SVC is in Dixon et al. 2018 and Orf et al. 2018.

Figure 5 shows the fully developed RFD occlusion for the Moore EF5 supercell at 19:51:11 Z. The RFD occlusion has reached a mature state and is ready to produce a tornado. All that is needed is for the DRC to infuse high winds into the RFD occlusion. DRC 1 is southwest of the RFD occlusion. When it wraps in, the low-level mesocyclone will stretch the column of vertical vorticity rapidly upward, and a tornado will be produced.

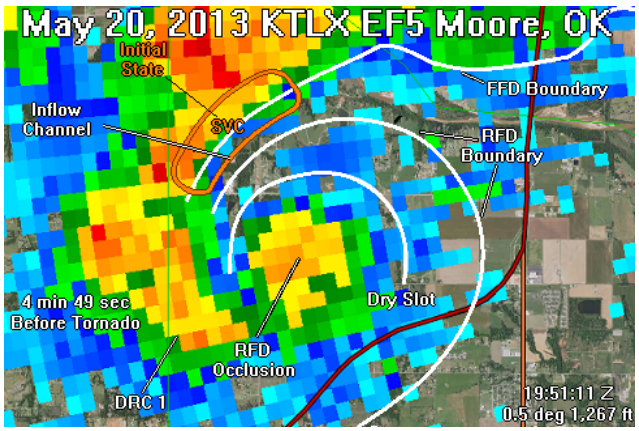

Figure 5. The fully developed RFD occlusion associated with the Moore EF5 supercell. The RFD occlusion matured at 19:51:11 Z, 4 minutes 49 seconds prior to the tornado start time. DRC 1 is just southwest of the RFD occlusion. The initial state SVC is northwest of the inflow channel.

Moore, Oklahoma EF5 Supercell at 19:52:53 Z - 3 Minutes 7 Seconds Before Tornado

RFD Occlusion Is Fully Matured - DRC 1 and Occlusion Downdraft Rapidly Descend Toward Surface Cells and Associated Outflow Approach from Southwest - Inflow Channel and SVC Develop

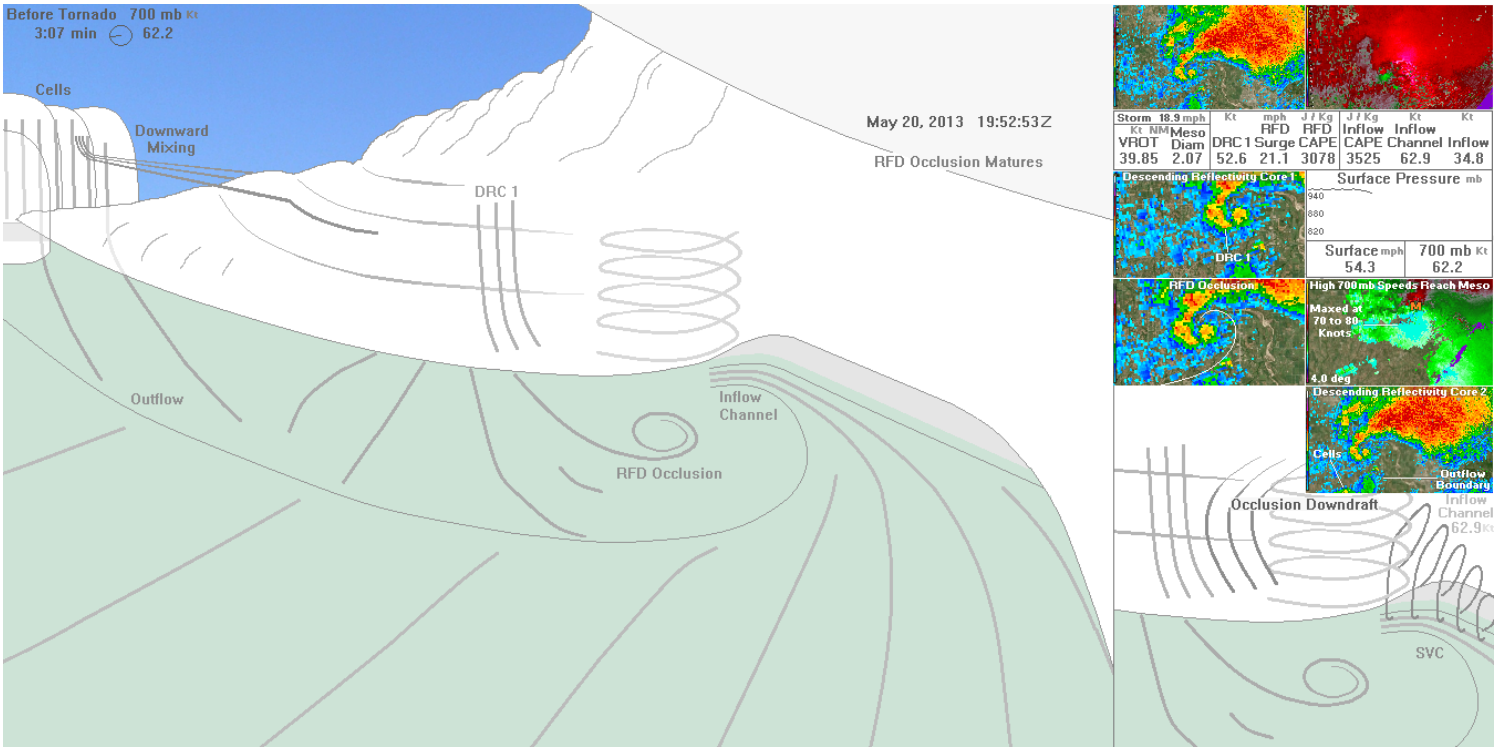

Figure 6. The Moore EF5 supercell at 19:52:53 Z. The RFD occlusion is fully matured. DRC 1 and the occlusion downdraft rapidly descend toward the surface (lower right insert). Cells approach the flanking line from the southwest. The inflow channel and associated SVC develop. The inflow channel peak wind speed has increased to 62.9 knots within the inflow channel, due to the Bernoulli Effect.

TORNADO FORMATION

Figure 7 shows the entire process of tornado formation for the Moore, Oklahoma EF5. Within that time series, the DRC (light gray) hits the ground (upper left two panels). The DRC and the occlusion downdraft (dark gray) combine during the descent. The funnel forms and lowers as the two features approach the center of the RFD occlusion (upper left three panels). A pressure deficit develops on the lee side of the nose of the DRC and occlusion downdraft, which allows the funnel to drop towards the surface. The tornado forms as the DRC wraps into the center of the RFD occlusion (upper fourth panel and Figure 8).

The Moore tornado grows steadily, reaching a diameter of 0.5 nautical miles and intensity of EF4 only 2 minutes 30 seconds after the tornado start time (bottom far left panel). The tornado continues to grow rapidly, reaching a peak width of 1.1 nautical miles 10 minutes after the tornado start time (bottom far right panel). This rapid increase in width and intensity is likely due to the remarkable organization of the supercell, and processes becoming favorably aligned.

The DRC appears to be critical to tornado formation because it infuses high winds into the RFD occlusion at ground-level, which greatly increases vertical vorticity. The DRC also provides a sheltering effect around the circulation, which allows vertical vorticity to organize without being torn apart by low-level vertical shear. The sheltering effect enables the pressure to drop on the lee side of the nose of the DRC.

As was presented in part 2 of this study, the 208 case average shows that the tornado forms as the leading edge of the DRC reaches the center of the RFD occlusion. If this occurs, a tornado is likely if the RFD is sufficiently unstable and the low-level mesocyclone is strong enough. A sample of DRCs is presented in Rasmussen et al. 2006.

Tornadogenesis Sequence for the Moore, Oklahoma EF5 Tornado on May 20, 2013

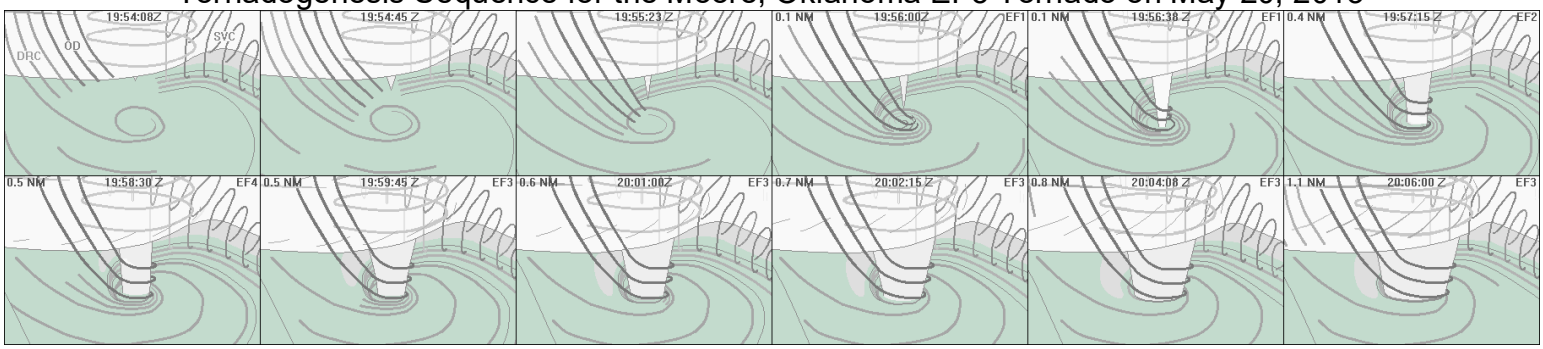

Figure 7. The process of tornadogenesis for the Moore EF5 supercell on May 20, 2013. The DRC (light gray) and occlusion downdraft (dark gray) descend to the surface and approach the RFD occlusion. The tornado develops as the DRC wraps into the center of the RFD occlusion. The tornado grows steadily, reaching 0.5 nautical miles in width and EF4 intensity only 2 minutes and 30 seconds after the tornado start time. The tornado reaches a maximum width of 1.1 nautical miles 10 minutes after the tornado starts, which is a testament of incredible organization.

Moore, Oklahoma EF5 Supercell at 19:56:00 Z - Start Time of Tornado

DRC Wraps Into RFD Occlusion As Tornado Begins - Cells Approach Flanking Line

Outflow Boundary Pushes Into Inflow Sector of Supercell South-southeast of Tornado

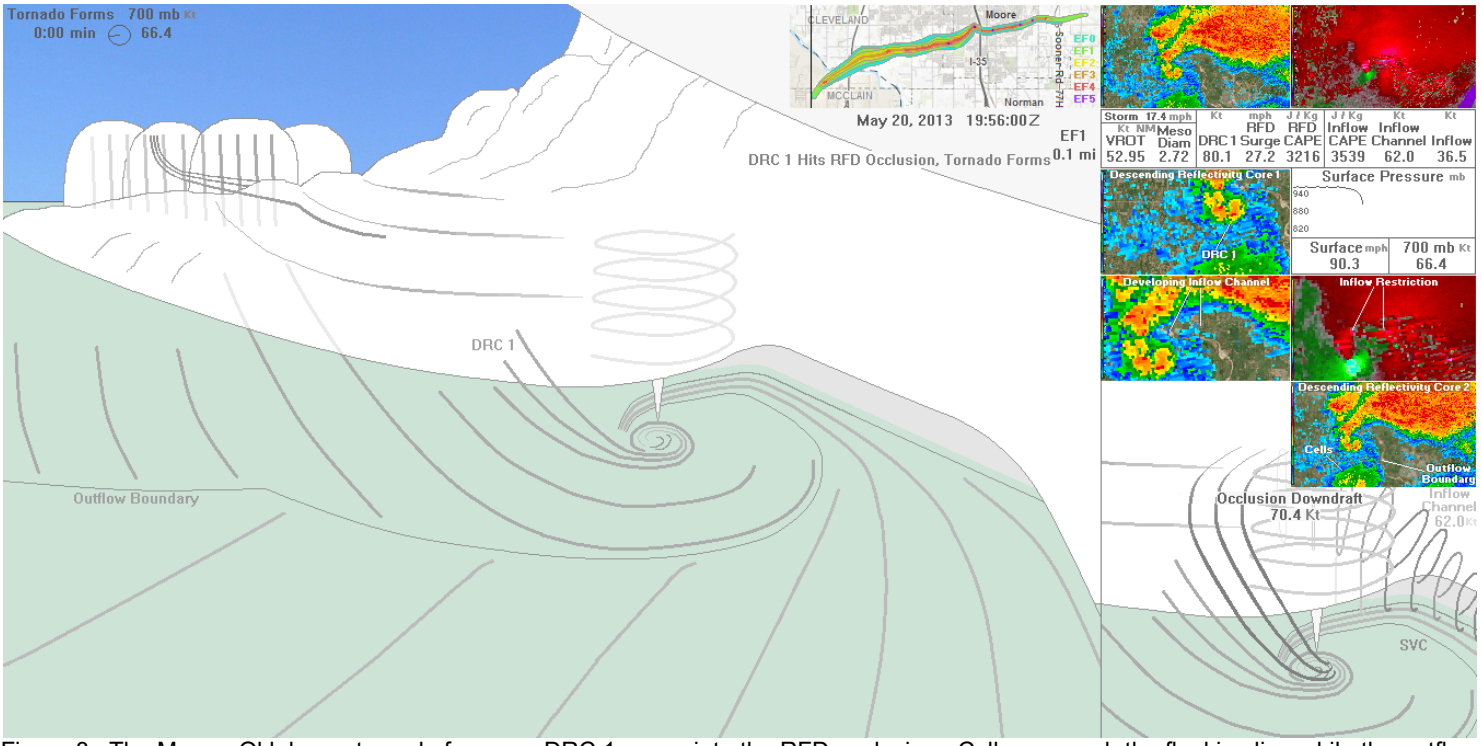

Figure 8. The Moore, Oklahoma tornado forms as DRC 1 wraps into the RFD occlusion. Cells approach the flanking line while the outflow boundary pushes quickly eastward into the inflow sector of the supercell.

SNAP-BACK PROCESS AND INTENSIFICATION TO EF5

In Figure 9, DRC 2 rapidly approaches the tornado from the southwest. DRC 2 instigates the second RFD surge and wraps into the tornado at 20:08:30 Z (upper right panel). At this time, tornado intensity increases to EF4. DRC 2 causes the RFD to expand outward toward the inflow channel. By 20:11:00 Z, the inflow channel is cut off (middle second panel). The second RFD surge reinforces the expansion of the surface mesocyclone around the tornado, with the meso reaching maximum size at 20:13:00 Z (middle fourth panel). From 20:14:45 Z to 20:17:15 Z, the low-level meso snaps back on the north side, with the diameter of the entire meso shrinking by 37 percent. As the surface mesocyclone becomes narrower, the contraction boosts the tornado to EF5 intensity for the first time.

Expansion and Snapback Process To EF5 Intensity for Moore, Oklahoma Tornado on May 20, 2013

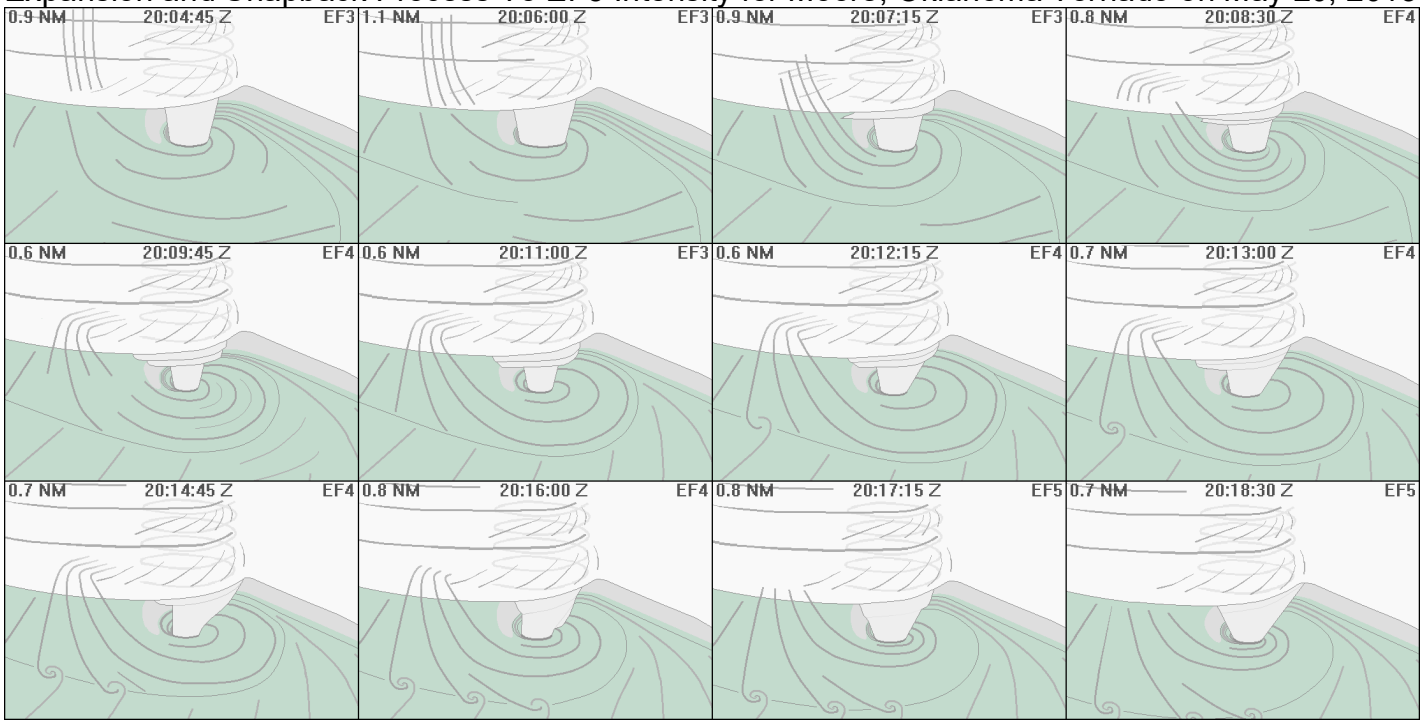

Figure 9. A process in which the RFD quickly expands as DRC 2 and the second RFD surge wrap into the surface mesocyclone surrounding the tornado (top four panels). The surface mesocyclone reaches maximum width at 20:13:00 Z (middle fourth panel) before a rapid contraction occurs. This snap back increases the tornado to EF5 intensity for the first time (lower right two panels).

In Figure 10, the tornado reaches a maximum width of 1.1 nautical miles in diameter. DRC 2 is approaching the tornado from the southwest, and will wrap around the RFD, resulting in a rapid expansion. The outflow from cells that earlier produced DRC 2, has stalled across the inflow sector. The outflow boundary is creating a long inflow channel.

Figure 11 shows DRC 2 wrapping around the tornado. A rapid expansion of the surface mesocyclone is occurring, which will soon cutoff the inflow channel. A process is occurring that is associated with violent tornadoes, in which the meso rapidly expands and shrinks, coinciding with tornado intensification. The second RFD surge has begun.

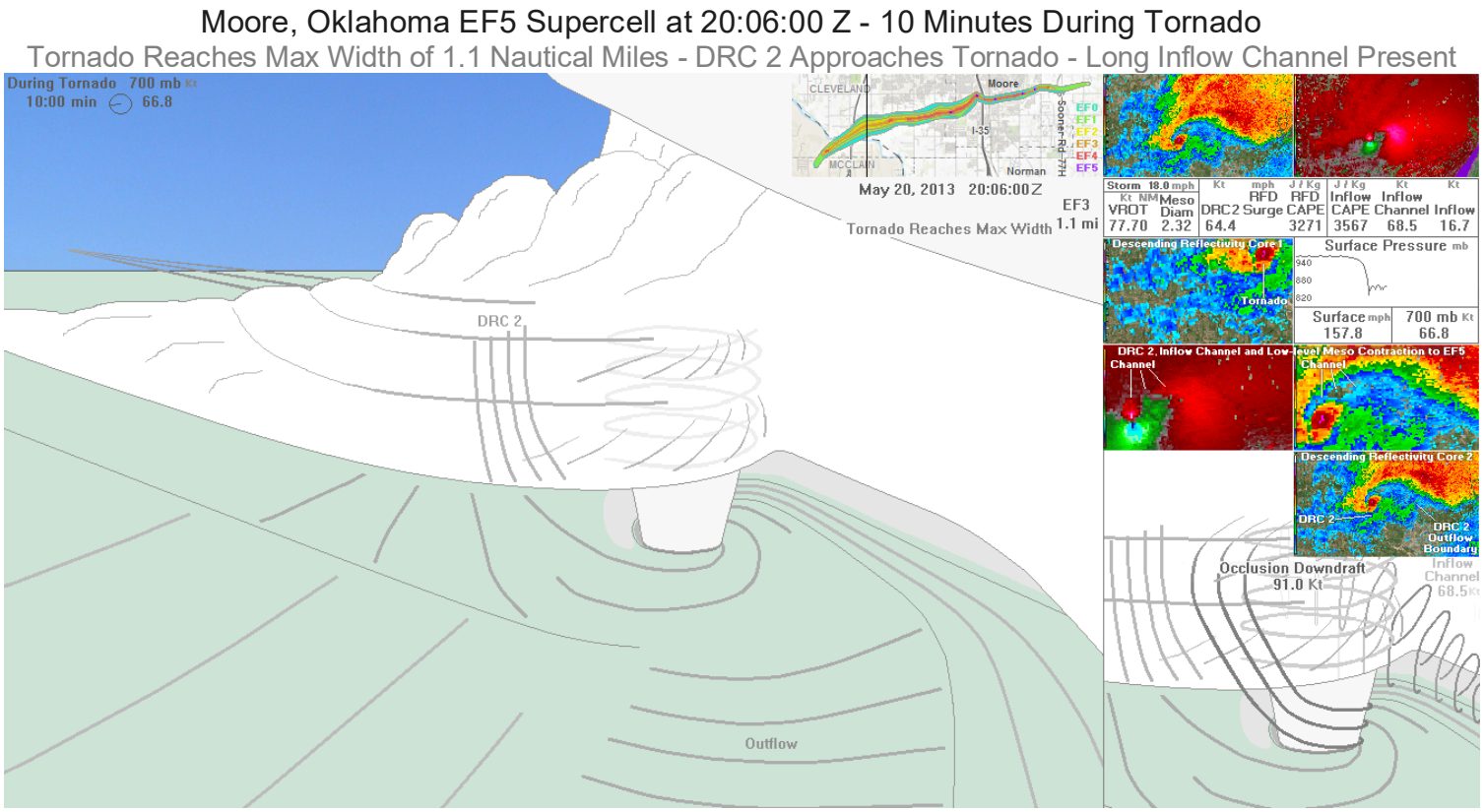

Figure 10. The tornado reaches maximum width of 1.1 nautical miles. DRC 2 approaches from the southwest and is descending toward the surface. The outflow boundary from cells that earlier produced DRC 2, stalls and creates a long inflow channel.

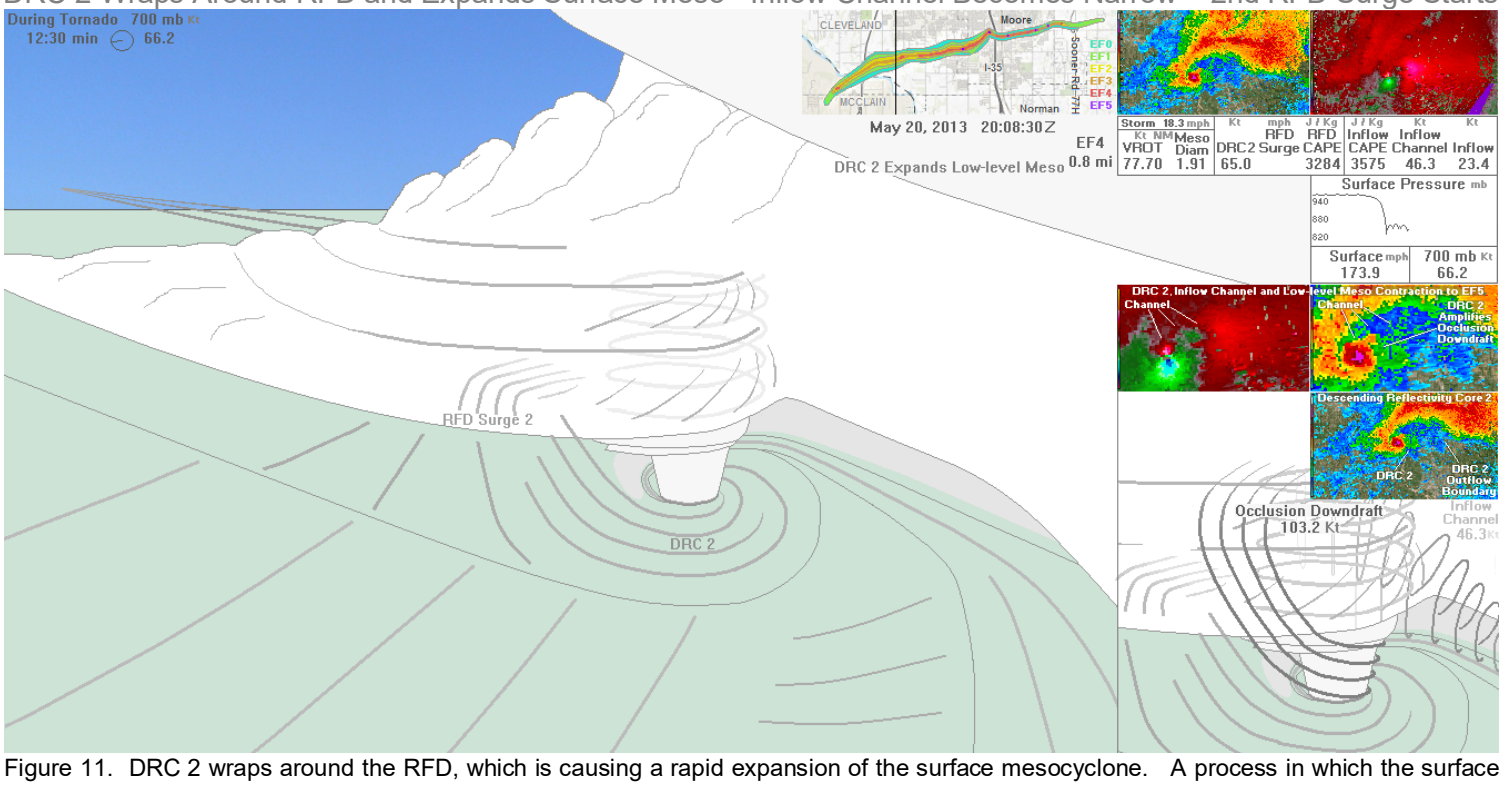

Figure 11. DRC 2 wraps around the RFD, which is causing a rapid expansion of the surface mesocyclone. A process in which the surface mesocyclone rapidly expands and contracts has begun, commonly associated with violent tornadoes. The second RFD surge is beginning. The outflow boundary from cells that earlier produced DRC 2, has stalled across the supercell's inflow sector creating a long inflow channel.

In Figure 12, the surface mesocyclone expansion, associated with DRC 2, has peaked. The inflow channel is blocked and the SVC has diminished. This happens before a rapid snap back occurs, coinciding with an increase in tornado intensity. Figure 13 shows the tornado after that snap back, reaching EF5 intensity for the first time. This expansion and snapback process for violent tornadoes is documented in Broyles et al. 2002.

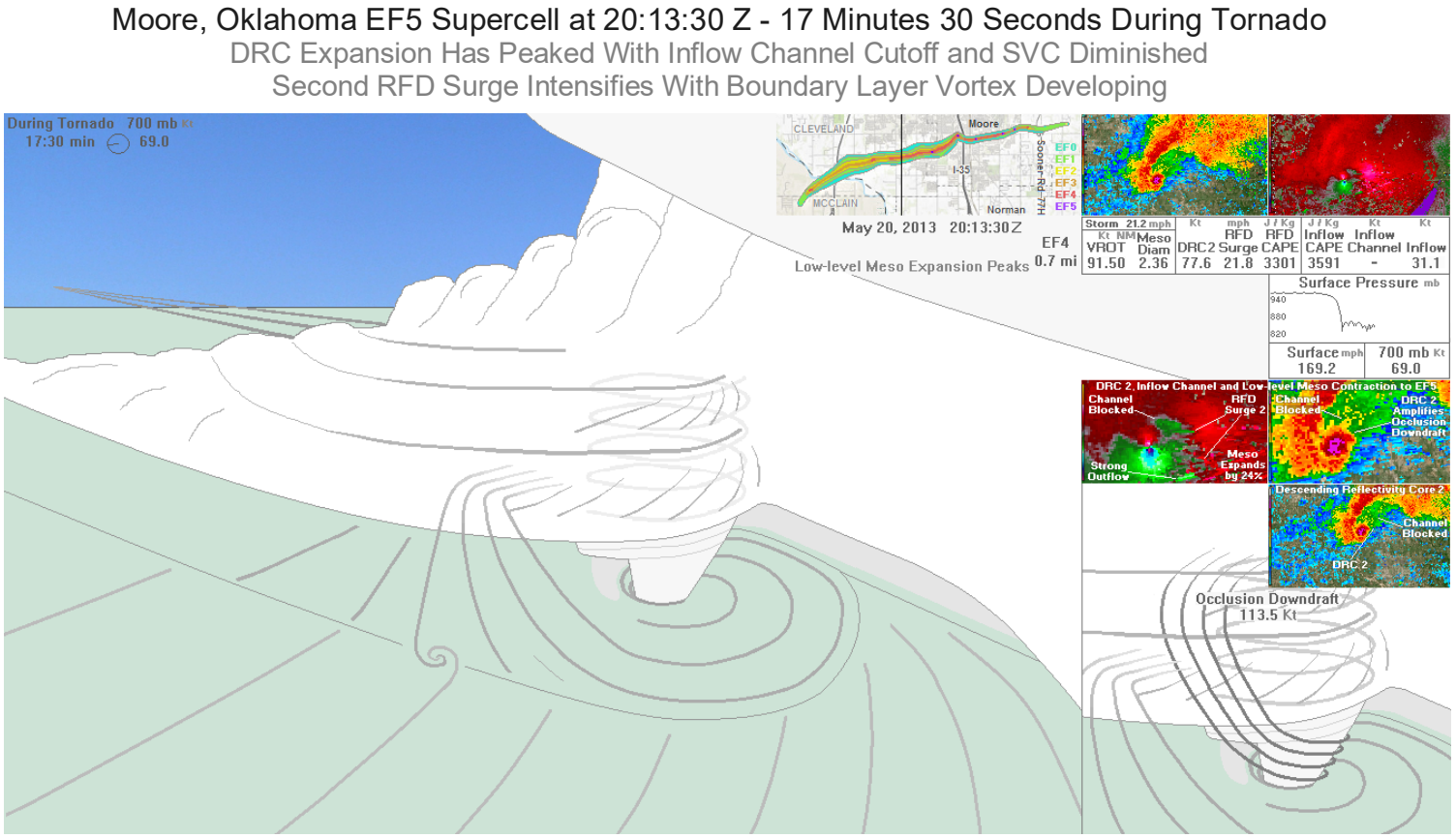

Figure 12. The expansion of the surface mesocyclone, associated with DRC 2, has maximized. The expanding RFD has cutoff the inflow channel, which has caused the SVC to diminish. A rapid snapback is about to occur which will result in a rapid intensification of the tornado. The second RFD surge is underway, which is resulting in boundary layer vortices that are starting to form on the RFD boundary.

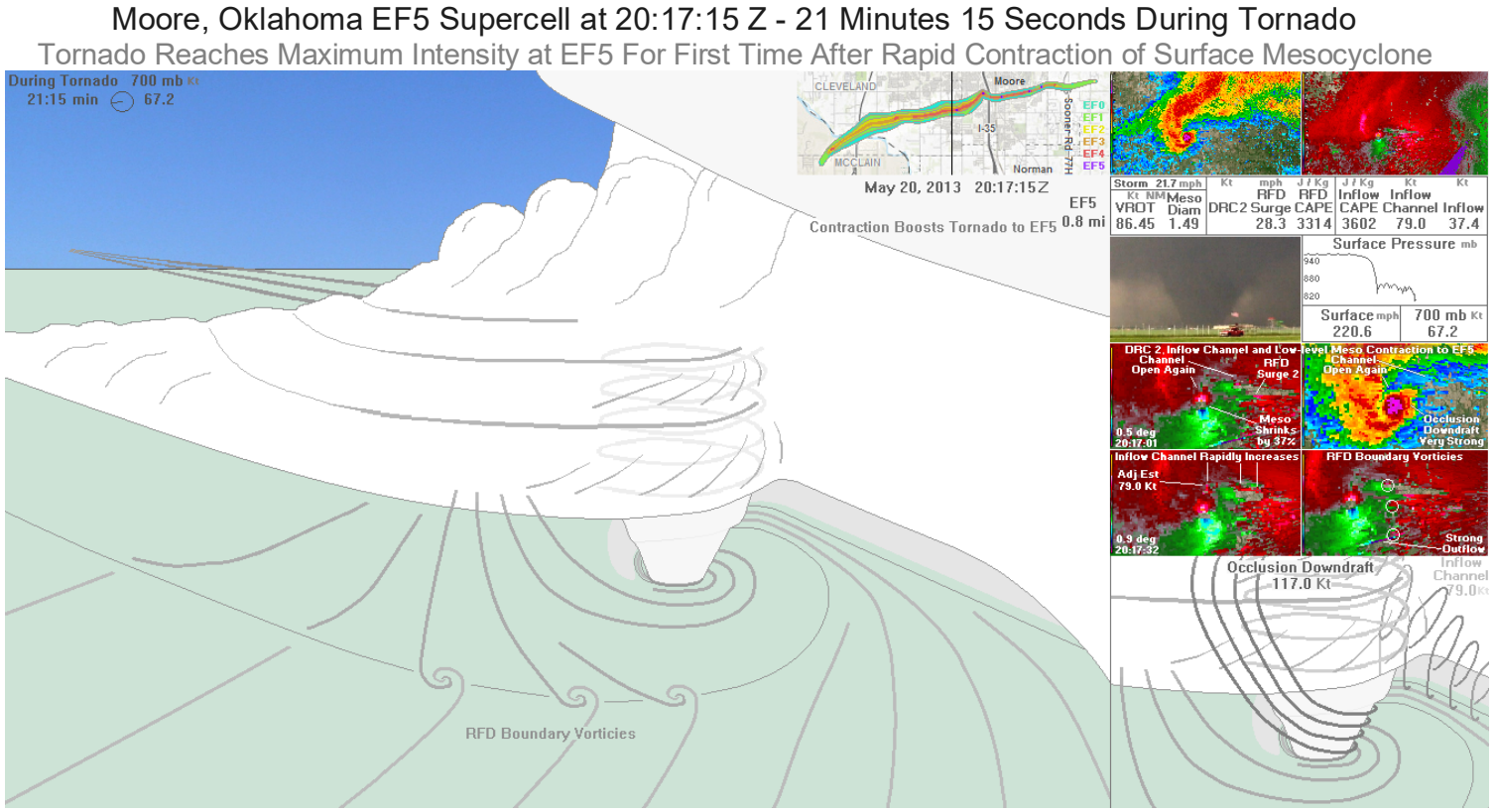

Figure 13. Tornado reaches peak intensity at EF5 for the first time after an expansion, and rapid contraction of the surface mesocyclone. The snap back coincides with an increase in inflow with wind speeds in the inflow channel peaking at 79 knots. The second RFD surge has caused low-level convergence to increase near the RFD boundary, along which three boundary-layer vortices have formed.

In Figure 13, the tornado reaches a maximum combination of width and intensity (0.8 nautical miles wide at EF5 intensity), caused by the rapid contraction of the low-level mesocyclone. During the contraction, the inflow channel reopens, and wind speeds in the channel peak at 79 knots.

Figure 14 shows that the meso-beta scale 700 mb jet has passed. The 700 mb wind speed impacting the flanking line, has decreased to 42 knots. As the 700 mb jet passes, the tornado shrinks by almost half. The tornado jogs northeastward before a sharp turn to the southeast.

Moore, Oklahoma EF5 Supercell at 20:23:30 Z - 27 Minutes 30 Seconds During Tornado

Meso-beta Scale 700 mb Jet Passes Flanking Line, Tornado Jogs Left and Then Right As Size Quickly Decreases

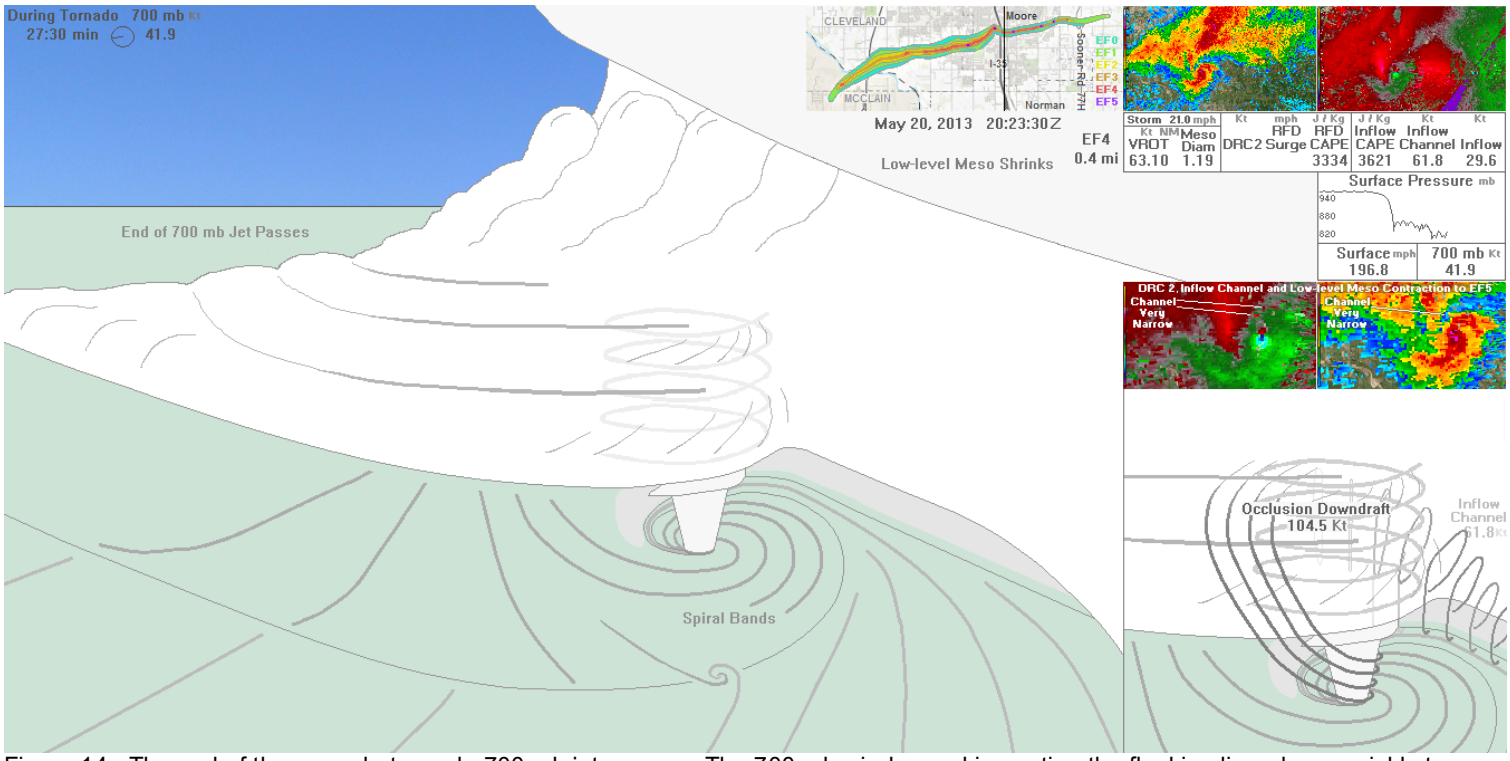

Figure 14. The end of the meso-beta-scale 700 mb jet passes. The 700 mb wind speed impacting the flanking line, drops quickly to near 42 knots. The passing of the 700 mb jet coincides with a sharp jog in the track. The tornado turns northeast and then back southeast. The tornado shrinks by almost half but remains intense, maintaining a violent rating. Spiral bands form around the tornado, evident on radar.

Moore, Oklahoma EF5 Supercell at 20:29:08 Z - 33 Minutes 8 Seconds During Tornado

Third RFD Surge Descends Toward Surface and Will Cause Tornado To Diminish

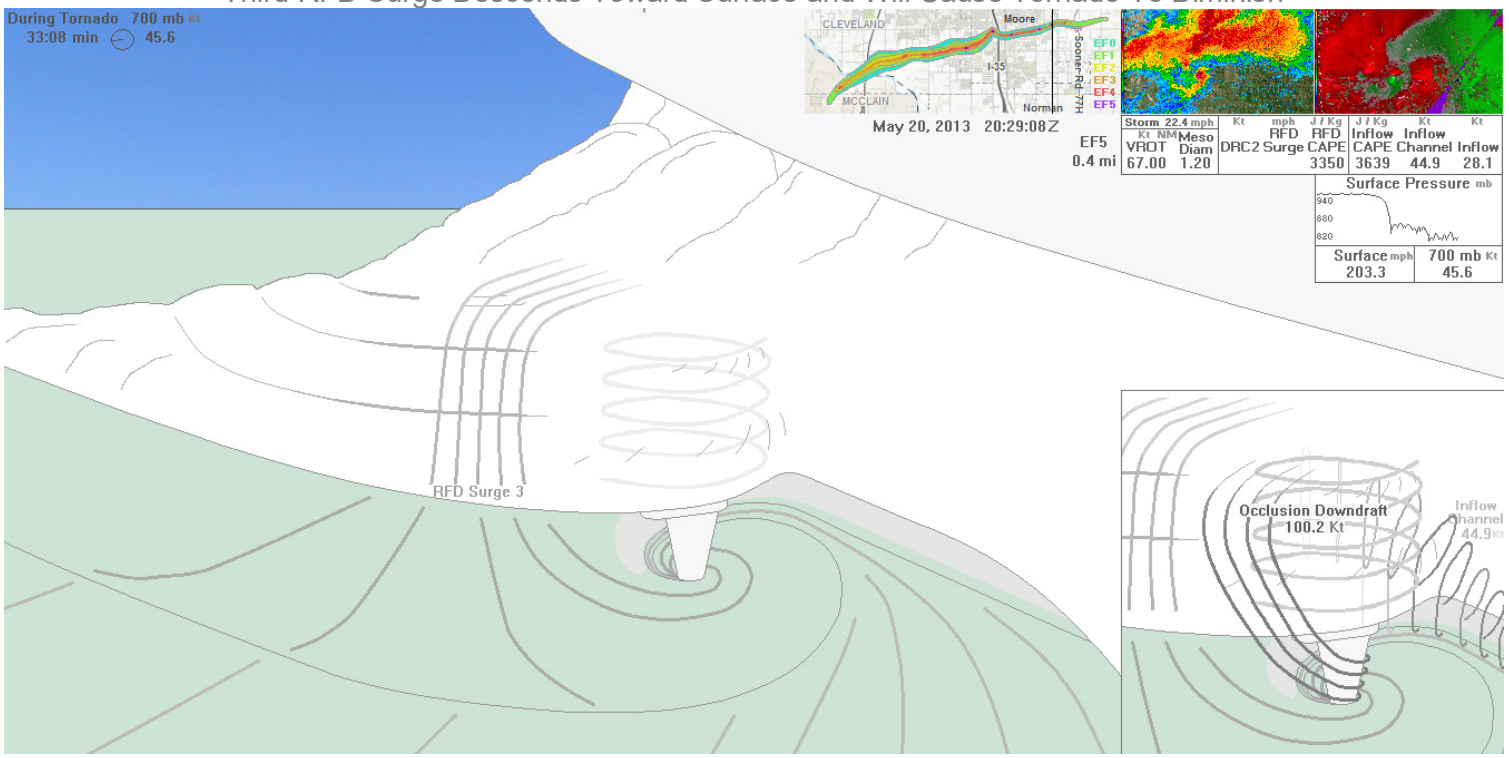

Figure 15. The third RFD surge descends to the surface at 20:29:08 Z. This will be the last time EF5 is observed with the Moore, Oklahoma supercell. This RFD surge originates high up within the supercell after the meso-beta scale 700 mb jet passes, which has weakened environmental flow. This RFD surge is relatively cool and stable. It will sweep underneath the low-level meso and cause the tornado to dissipate.

In Figure 15, the third RFD surge is rapidly descending within the flanking line at 20:29:08 Z. This RFD surge originates higher up in the storm due to the passing of the meso-beta scale 700 mb jet. This is the last time the tornado will be observed at EF5 intensity. In spite of the relatively weak 700 mb wind speed of 46 knots, the supercell remains strong because it takes time for the highly organized storm to unwind. The last time that a violent tornado is observed with the Moore supercell is 20:31:00 Z, 9 minutes after the passing of the meso-beta scale 700 mb jet. From this point, the Moore tornado will begin a weakening cycle. In Figure 16, the tornado is about to end. The Moore tornado officially diminishes at 20:35:00 Z, 39 minutes after the tornado began.

Moore, Oklahoma EF5 Supercell at 20:34:45 Z - 38 Minutes 45 Seconds During Tornado

Third RFD Surge Pushes Toward Tornado and Will Cause Tornado To Dissipate In 15 Seconds

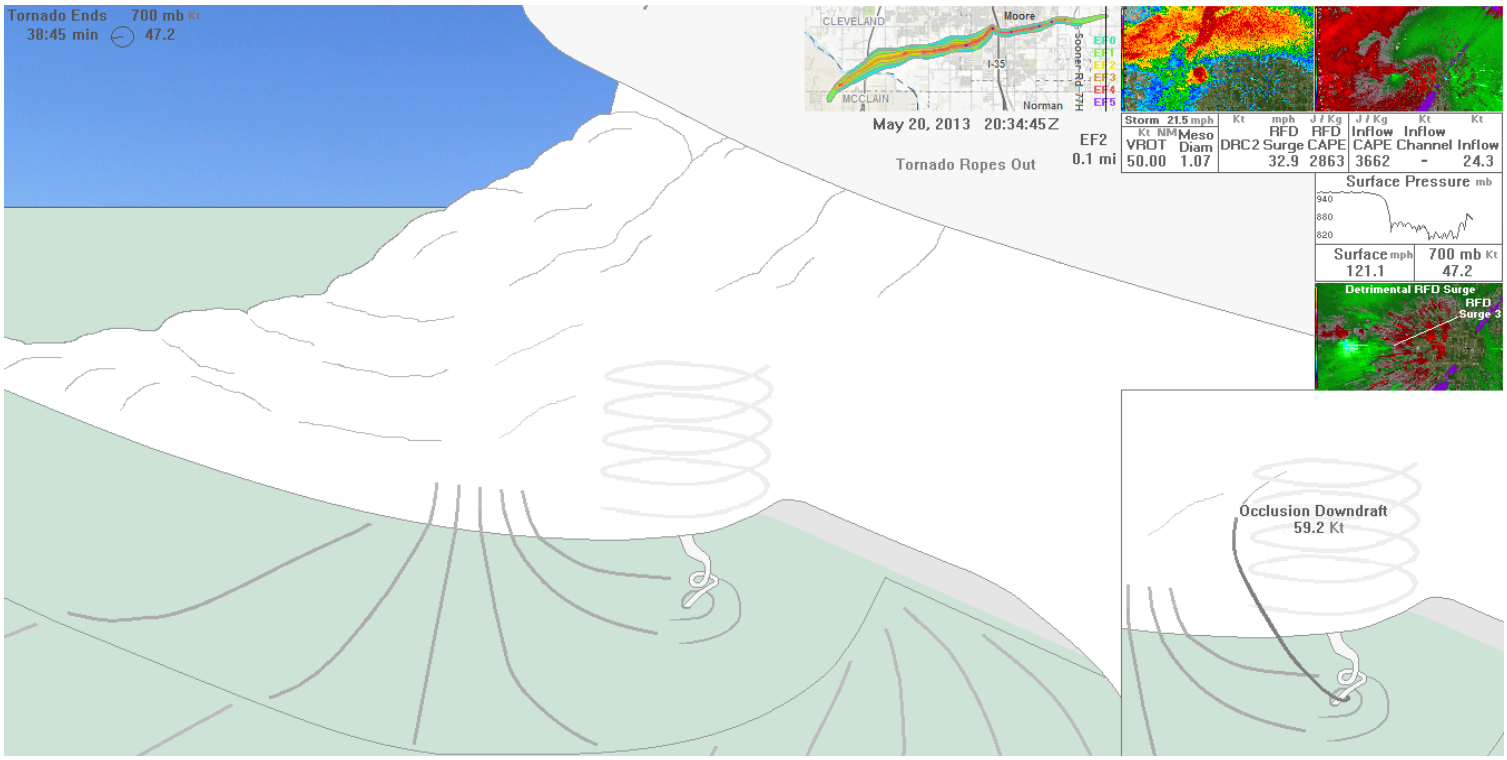

Figure 16. At 20:34:45 Z, the third RFD surge pushes toward the tornado and will cause the tornado to dissipate in 15 seconds.

4. FINAL CONSIDERATIONS

Throughout this study in Part 1 to 3, measurements were made using base velocity in order to estimate wind speeds in different areas of the supercell and at different elevations around the supercell. A method to correct the estimated wind speed was used based on the estimated wind speed direction relative to the beam direction. Streamlines in and around the supercell, based on reflectivity and supercell structure theory, were drawn to estimate the wind directions. The wind speed estimates using base velocity were obtained from the bin associated with the estimate. While this technique is new, it does provide a way to gather wind speed data from within and around the supercell. We acknowledge that the obtained wind speed data are estimates, and that error is present. However, the resulting wind speeds seem reasonable in estimating the environmental flow in and around the supercell.

5. CONCLUSION

At the start of this project, 208 supercells with EF3 to EF5 tornadoes were entered onto a spreadsheet to be examined. Data for events associated with tornadogenesis were gathered for each storm and entered on the spreadsheet. During the analysis phase of the project, the pandemic slowed progress. At the start of October 2020, only 26 storms had been analyzed. At that time, a side project related to tornadogenesis began. The goal was to create an animation showing processes commonly associated with tornadogenesis based on the data gathered. The database average start and end times for each event surrounding tornadogenesis would be used to draw the process leading up to the tornado.

After the first version of the animation was complete, the Moore, Oklahoma EF5 supercell on May 20, 2013 was examined and appeared to be close to the average, which would make it easier to adapt the animation.

In the fall of 2021, analysis was started again to make progress on the 208 supercell database. After 60 supercells had been analyzed, an algorithm was developed in order to rank each storm according to how close it was to the database average. By early spring 2022, the analysis for the 208 case database was complete, and the Moore EF5 supercell was the closest to the 208 case average. This confirmed to the authors that the Moore EF5 supercell was representative of the processes involved in tornadogenesis for this dataset.

The animation consists of 227 frames, with 37.5 seconds between frames. The animation spans 2 hours 21 minutes 15 seconds, showing the initial cloud development of the Moore EF5 supercell continuing through the complete tornado cycle of the Moore EF5 tornado.

Shortly after the animation begins, the Moore EF5 supercell initiates as a tiny cloud on the horizon, looking north-northwest. The cloud grows steadily in size. 20 minutes after convective initiation, the Moore storm becomes a supercell with a strengthening mesocyclone. The viewing

direction gradually turns toward the west as the Moore supercell develops. 40 minutes into the storm, a strong low-level mesocyclone is present.

Cell initiation takes place at 19:26:00Z, just behind the flanking line. The two developing cells merge at 19:38:30.Z. This instigates the RFD surge 3 minutes 45 seconds later, at 19:42:15 Z (13 minutes 45 seconds prior to tornado start time).

At 19:42:15 Z, a meso-beta scale 700 mb jet hits the flanking line of the Moore EF5 supercell. This increases the 700 mb wind speed from 46.6 knots to 72.1 knots in 5 minutes 37 seconds. This rapid increase in wind speed causes the storm to rapidly rotate and strengthens the low-level mesocyclone dramatically. The RFD occlusion begins to develop within the northeast quadrant of the RFD at 19:47:15 Z. The RFD surge is strengthened as well, pushing north and east toward the forward flank of the supercell.

The RFD surge causes the inflow channel to develop at 19:51:00 Z, five minutes prior to the tornado start time. DRC 1, a result of the cell merger, approaches the low-level mesocyclone from the west-southwest. DRC 1 and the occlusion downdraft descend toward the surface just prior to the tornado start time. The tornado forms as the nose of DRC 1 wraps into the center of the RFD occlusion.

The descending reflectivity core appears to be critically important to tornadogenesis because it infuses high winds into the RFD occlusion, greatly strengthening vertical vorticity. The DRC also likely provides a sheltering effect, protecting the developing column of vertical vorticity from being torn apart by low-level vertical shear.

After the Moore tornado formed, it quickly strengthened, reaching EF4 status 2 minutes 30 seconds after the tornado start time. It reached a maximum width of 1.1 nautical miles 10 minutes after the tornado start time. This incredibly rapid development was likely due to the high-end organization that the Moore EF5 supercell displayed.

DRC 2 approaches the Moore tornado from the southwest, and wraps around the tornado at 20:08:30 Z. Simultaneously, the low-level mesocyclone quickly expands. The expansion is reinforced by the second RFD surge. After the expansion, a snap-back occurs when the low-level mesocyclone decreases by 37 percent in just 4 minutes and 15 seconds. This shrinking occurred primarily on the northern side of the low-level mesocyclone, as the inflow channel reopened. At this time, the Moore tornado reaches EF5 status for the first time. This expansion and snap-back process has been observed for tornadoes that strengthen into the violent category.

At 20:23:30 Z, the meso-beta scale 700 mb jet passes. As a result, 700 mb wind speeds decrease from 70 knots to 41.9 knots in just 7 minutes 8 seconds. This coincides with a jog in the tornado track, first to the northeast, and then to the southeast. After the passing of the 700 mb jet, wind speeds at low to mid-levels within the storm weaken, allowing an RFD surge to originate up high in the Moore EF5 supercell. This third RFD surge is relatively cool and stable. This RFD surge overtakes the tornado at 20:35:00 Z, 39 minutes after to the tornado began.

The Moore EF5 supercell shows us the complexity of tornadogenesis. Multiple processes happened at just the right times, working together. These processes interacted in a way that allowed a high-end tornado to form. The processes involved in tornado development are displayed in the animation of the Moore EF5 supercell.

Hopefully, the animation will help many to better understand tornadogenesis for high-end tornadic supercells. The animation is on the Storm Prediction Center website at https://www.spc.noaa.gov/publications/broyles/m13-anim.pptx. The presentation that was made at the Severe Local Storms conference in October 2023, is available at https://www.spc.noaa.gov/publications/broyles/m13-talk.pptx. Both PowerPoint presentations are located in the Conference Papers section under Broyles next to the listing for this paper.

For questions about this study, please contact Chris Broyles at chris.broyles@noaa.gov.

6. ACKNOWLEDGEMENTS
We are extremely grateful to Israel Jirak for doing an excellent review of our papers. We are also thankful to the guidance that Patrick Skinner gave to us early on during our tornadogenesis project. Thanks also goes to John Hart and Brian Squitieri for giving guidance during the review process. Also, we are thankful to Paul Markowski and Jana Houser, who we consulted early in the project for guidance. Finally, we thank Ethan Broyles for giving us feedback concerning graphic presentation.

7. REFERENCES

Atkins, N. T., Butler K. M. , Flynn K. R. , and Wakimoto R. M. , 2014: An integrated damage, visual, and radar analysis of the 2013 Moore, Oklahoma, EF5 tornado. *Bull. Amer. Meteor. Soc.*, **95**, 1549–1561

Browning, K. A., 1964: Airflow and precipitation trajectories within severe local storms which travel to the right of the winds. *J. Atmos. Sci.,***21,** 634–639.

Browning, K. A., and F. H. Ludlam, 1962: Airflow in convective storms. *Quart. J. Roy. Meteor. Soc.*, **88 ,** 117–135.

Browning, K. A., and R. J. Donaldson, 1963: Airflow and structure of a tornadic storm. *J. Atmos. Sci.*, **20 ,** 533–545.

Broyles, C., R. Wynne, N. Dipasquale, H. Guerrero, T. Hendricks, 2002: Radar characteristics of violent tornadic storms using the NSSL algorithms across separate geographic regions of the United States. Preprints, *21st Conf. on Severe Local Storms,* San Antonio, TX, Amer. Meteor. Soc., 5.1

Burgess, D., K. Ortega, G. Stumpf, G. Garfield, C. Karstens, T. Meyer, B. Smith, D. Speheger, J. LaDue, R. Smith, and T. Marshall, 2014: 20 May 2013 Moore, Oklahoma, tornado: Damage survey and analysis. *Wea. Forecasting*, **29**, 1229–1237.

Davies-Jones, R. P., 2006: Tornadogenesis in supercell storms—What we know and what we don't know. Preprints, *Symposium on the Challenges of Severe Convective Storms,* Atlanta, GA, Amer. Meteor. Soc., 2.2.

Dixon, A., L. Orf, and K. Halbert, 2018: The streamwise vorticity current: Its origin and strategies for remote detection. *29th Conf. on Severe Local Storms*, Stowe, VT, Amer. Meteor. Soc.,84.

Finley, C. A., B. D. Lee, M. Grzych, C. D. Karstens, and T. M. Samaras, 2010: Mobile mesonet observations of the rear-flank downdraft evolution associated with a violent tornado near Bowdle, SD on 22 May 2010. Preprints, *25th Conf. on Severe Local Storms,* Denver, CO, Amer. Meteor. Soc., 8A.2.

Klemp, J. B., and R. Rotunno, 1983: A study of the tornadic region within a supercell thunderstorm. *J. Atmos. Sci.,* **40,** 359–377.

Kosiba, K., A. J. Wurman, P. Markowski, Y. Richardson, P. Robinson, and J. Marquis, 2013: Genesis of the Goshen County, Wyoming, tornado on 5 June 2009 during VORTEX2. *Mon. Wea. Rev.*, **141**, 1157-1181.

Kurdzo, J. M., Bodine D. J. , Cheong B. L. , and Palmer R. D. , 2015: High temporal resolution polarimetric X-band Doppler radar observations of the 20 May 2013 Moore, Oklahoma Tornado. *Proc. 27th Conf. on Severe Local Storms,* Madison, WI, Amer. Meteor. Soc., 11A.3.

Lee, B. D., C. A. Finley, and C. D. Karstens, 2012: The Bowdle, South Dakota, cyclic tornadic supercell of 22 May 2012: Surface analysis of rear-flank downdraft evolution and multiple internal surges. *Mon. Wea. Rev.*, **140,** 3419–3441.

Lemon, L. R. and C. A. Doswell, 1979: Severe thunderstorm evolution and mesocyclone structure as related to tornadogenesis. *Mon. Wea. Rev.*, 107, 1184-1197.

Markowski, P. A., 2002a: Hook echoes and rear-flank downdrafts: A review. *Mon. Wea. Rev.*, **130 ,** 852–876.

Orf, L., R. Wilhelmson, A. Dixon, T. Halbert, 2018: The Role of the Streamwise Vorticity Current in Tornado Genesis and Maintenance. *Preprints, 29th Conf. on Severe Local Storms*, Stowe, VT, Amer. Meteor. Soc., 1.5.

Ortega, K., D. Burgess, G. Garfield, C. Karstens, J. LaDue, T. Marshall, T. Meyer, B. Smith, R. Smith, D. Speheger, and G. Stumpf, 2014: Damage survey and analysis of the 20 May 2013 Newcastle–Moore EF-5 tornado. *Special Symp. on Severe Local Storms: The Current State of the Science and Understanding Impacts,* Atlanta, GA, Amer. Meteor. Soc., 828.

Rasmussen, E. N., J. M. Straka, M. S. Gilmore, and R. P. Davies-Jones, 2006: A preliminary survey of rear-flank descending reflectivity cores in supercell storms. *Wea. Forecasting*, **21**, 923–938.

Satrio, C. 2019: Multi-Radar Analysis of the 20 May 2013 Moore, Oklahoma Supercell through Tornadogenesis and Intensification, Thesis, University of Oklahoma

Wurman, J., Y. Richardson, C. Alexander, S. Weygandt, P. F. Zhang, 2007: Dual-Doppler and Single-Doppler Analysis of a Tornadic Storm Undergoing Mergers and Repeated Tornadogenesis. *Mon. Wea. Rev.*, **135**, 736-758.